Supplementary Files for *Machine Learning Based Prediction of Small Intracranial Aneurysm Rupture Status Using Computed Tomography Angiography Derived Hemodynamics: A Multicenter Study.*

Appendices

Figures

Tables

Supplemental Table 5. Performance of 3 ML Models to Predict Rupture Status of small Aneurysms in the Training, Internal Validation and External Validation Datasets.

Supplemental Appendix 1. Introduction of the Hemodynamic Parameters by CFD.

Eleven quantitative hemodynamic parameters were included in this study to describe and analyze the sophisticated blood flow conditions. The parameters were pressure, wall shear stress (WSS), averaged WSS-absolute (AWSS-ABS), averaged WSS-mean (AWSS-MEAN), WSS gradient (WSSG), averaged WSS gradient (AWSSG), oscillatory shear index (OSI), relative residence time (RRT), aneurysm formation index (AFI), gradient oscillatory number (GON) and spatial WSS gradient (G). All parameter values were acquired from cardiac systolic telophase.[1,2] The amount of each quantitative hemodynamic factor depends on the amount of image-based aneurysm grid, therefore we used the coefficient of variation (CV) which could describe the dispersion degree of data to describe the hemodynamic parameters of intracranial aneurysms sac. In the following, the quantitative hemodynamic parameters were expressed as $Pressure_{CV}$, $AWSSMEAN_{CV}$, WSS_{CV}, $AWSSABS_{CV}$, OSI_{CV}, RRT_{CV}, $WSSG_{CV}$, $AWSSG_{CV}$, AFI_{CV}, G_{CV}, and GON_{CV}.

Quantitative hemodynamic parameters

1. Pressure.
2. Wall shear stress (**WSS**): WSS is the tangential force exerted by the viscosity of the movement of the blood wall. It is measured in N/m^2, namely in Pa.
3. Averaged WSS- absolute (**AWSS-ABS**): time-average of the absolute value of WSS during a cardiac cycle.
4. Averaged WSS -mean (**AWSS-MEAN**): time-average of the mean WSS during a cardiac cycle.
5. WSSgradient (**WSSG**): a spatial derivative measure along the direction of the flow.
6. Averaged WSSgradient (**AWSSG**): the time-average spatial WSS gradient during a cardiac cycle.
7. Oscillatory shear index (**OSI**): a non-dimensional parameter, means the directional change of WSS during the cardiac cycle.
8. Relative residence time (**RRT**): a marker of disturbed flow, which marked by low magnitude and high oscillatory wall shear stress.
9. Aneurysm formation index (**AFI**): quantifies the cosine of the angle between two vectors, which represent a certain instant during the flow cycle and the time-averaged WSS vector.
10. Gradient oscillatory number (**GON**): quantifies the degree of oscillating tension/compression forces.

11. **G**: spatial WSS gradient.

Qualitative hemodynamic parameters

Four qualitative hemodynamic parameters were included in this study. The parameters were consisted of flow complexity, flow stability, inflow concentration, flow impingement introduced by Cerebral et al.[3] The computed blood flow fields were visualized by using streamlines in the sac.

The hemodynamic visualizations were analyzed to classify blood flows according to the following characteristics:

Flow complexity. "Simple" flow pattern indicates flow patterns consisting of a single recirculation zone or vortex structure within the aneurysm. "Complex" indicates flow patterns exhibiting flow divisions or separations within the aneurysm sac and containing more than 1 recirculation zone or vortex structure.

Flow stability. "Stable" indicates flows patterns that persist (do not move or change) during the cardiac cycle. "Unstable" indicates flow patterns in which the flow divisions and/or vortex structures move or are created or destroyed during the cardiac cycle.

Inflow concentration. "Concentrated" inflow streams or jets penetrate relatively deep into the aneurysm sac and are thin or narrow in the main flow direction. "Diffuse" indicates inflow streams that are thick compared with the aneurysm neck and flow jets that disperse.

Flow impingement. The "flow impingement zone" is the region of the aneurysm where the inflow stream is seen to impact the aneurysm wall and change its direction and/or disperse. Typically this region has an associated region of elevated WSS: a small impingement if the area of the impingement region is small compared with the area of the aneurysm (<50%); a large impingement, if the area of impingement is large compared with the area of the aneurysm (>50%).

For the evaluation of qualitative hemodynamic parameters, an inter-reader agreement analysis was performed. 200 aneurysms in the training cohort were randomly selected and evaluated independently by two observers (G.Z.C. and Z.S., with 7 and 3 years experiences in neuroradiology, respectively), who were blinded to the clinical history of the patients. In cases of disagreement between the two observers, consensus was reached after a joint reading. After validating good inter-reader agreement, the qualitative hemodynamic assessment of all aneurysms was performed by an observer (G.Z.C. with 7 years experiences in neuroradiology).

Supplementary Figure 2 shows some representative qualitative hemodynamic images for

unruptured and ruptured intracranial aneurysms.

Supplemental Appendix 2. Introduction of the Employed Machine Learning Algorithms.

Four ML methods (LR, SVM, RF, and MLP) for developing a prediction model were implemented for predicting small intracranial aneurysms rupture status, and they represent different categories of ML algorithm. The details of the methods are as follows:

Logistic Regression (LR): LR model is a regression model. For each data sample, the LR model will output the probability of being positive. In the training stage, the goal of the model is to estimate a weight for each data dimension to minimize the differences between prediction and label. This weight matrix can tell us how each data dimension will influence the final prediction and this is why LR model has good interpretability.

Support Vector Machine (SVM): SVM is a binary classification model. For each data sample, the SVM model will output distance between current data sample, the sign symbol of this distance indicate prediction is positive or negative. The goal of this model in training stage is to find a linear hyperplane separating positive data samples from negative data samples in training set with maximum margin. Besides, we applied kernel function to SVM model to map data into higher dimension to make more accurate hyperplane.

Random Forest (RF): The RF model is an ensemble algorithm. RF model consist of a collection of regression or classification decision trees. In training stage, this model is to fit these trees to data. And in prediction stage, the model will output the average prediction of trees in the forest. More details about random forest model can be found in original article.[4]

Multi-layer perceptron (MLP): MLP model is a regression model. The implanted MLP is a three-layer network, consists of an input layer, a 64-unit hidden layer and an output layer. Activation function of this network is Rectified Linear Unit (RELU), and the optimizer is Adam. The introduction of this hidden layer will make the MLP model better use data and achieve better performance.

Supplemental Appendix 3. Introduction of the Employed Feature Selection Algorithms.

There were 6 methods used for feature selection in our study, which can be divided into filter (F-test, Pearson correlation coefficient based, mutual information-based feature selection algorithms), wrapper (Recursive Feature Elimination (RFE) algorithm) and embedded categories (L1 based and tree-based feature selection algorithms). Each method was employed individually, and the method with the highest AUC in the validation set was selected.

The filter feature selection methods apply a statistical measure to calculate scores of features, and rank scores to decide whether this feature should be removed or not. In this study, F-test, Pearson correlation coefficient and mutual information-based feature selection algorithms were conducted. Each of the three filter feature selection methods was set to preserve 1%, 5%, 10%, 30% and 50% of the features, so a total of 15 filtering feature selection methods were tested.

For wrapper methods, different feature combinations of features were prepared and selected by the final performance of a base model. RFE algorithm was employed and a 5-fold cross validated Logistic Regression (LR) model was used as base model. Considering matching the number of features, the step size of RFE was set to 10 and the half of the features were selected.

Embedded method prefers to choose the features that best contribute to the accuracy of the base model. In our study, L1 based and tree-based feature selection algorithms were tried. The L1 based method used linear C-support vector classification model as base model, and 4 penalization intensity was tested (C=0.01, 0.1, 1 and 10). The tree-based feature selection algorithm employed extra-trees classifier as base model (num of estimators = 100, criterion = gini, min samples for split = 2, min samples per leaf = 1, min impurity decrease = 0.0). Above all, 5 embedded methods were tested in our study.

Supplemental Appendix 4. The Feature Selection Results

The features used for models fitting are described below:

Logistic Regression (LR):

Clinical: age; sex of male; with smoke; with diabetes mellitus; with ischemic stroke; with coronary artery disease;

Morphological: size; with regular shape; with unregular shape; locate at PCoA; locate at ACoA; locate at ICA; locate at MCA;

Hemodynamic: with stable inflow; with concentrated inflow concentration; with small impingement area; with hypertension; WSS; RRT; OSI; GON; AWSSG.

Support Vector Machine (SVM)：

Clinical: age; sex of male; with smoke; with alcohol intaking; with diabetes mellitus; with coronary artery disease; with ischemic stroke;

Morphological: size; with unregular shape; locate at PCoA; locate at ACoA; locate at ICA; locate at MCA; without daughter sac; with single aneurysm; with simple flow pattern in the aneurysm sac;

Hemodynamic: with stable inflow; with concentrated inflow concentration; with small impingement area; with hypertension; pressure; OSI; RRT; WSS; AWSSG; AWSSMEAN; GON; WSSG; AFI; AWSSABS; G.

Random Forest (RF):

Clinical: age; sex of male; with smoke; with diabetes mellitus; with coronary artery disease; with ischemic stroke;

Morphological: Size; with unregular shape; locate at PCoA; locate at ACoA; locate at ICA; locate at MCA;

Hemodynamic: with stable inflow; with concentrated inflow concentration; with small impingement area; WSS; GON; OSI; RRT; AWSSG; with hypertension.

Multi-layer Perceptron (MLP):

All collected features were involved for model fitting.

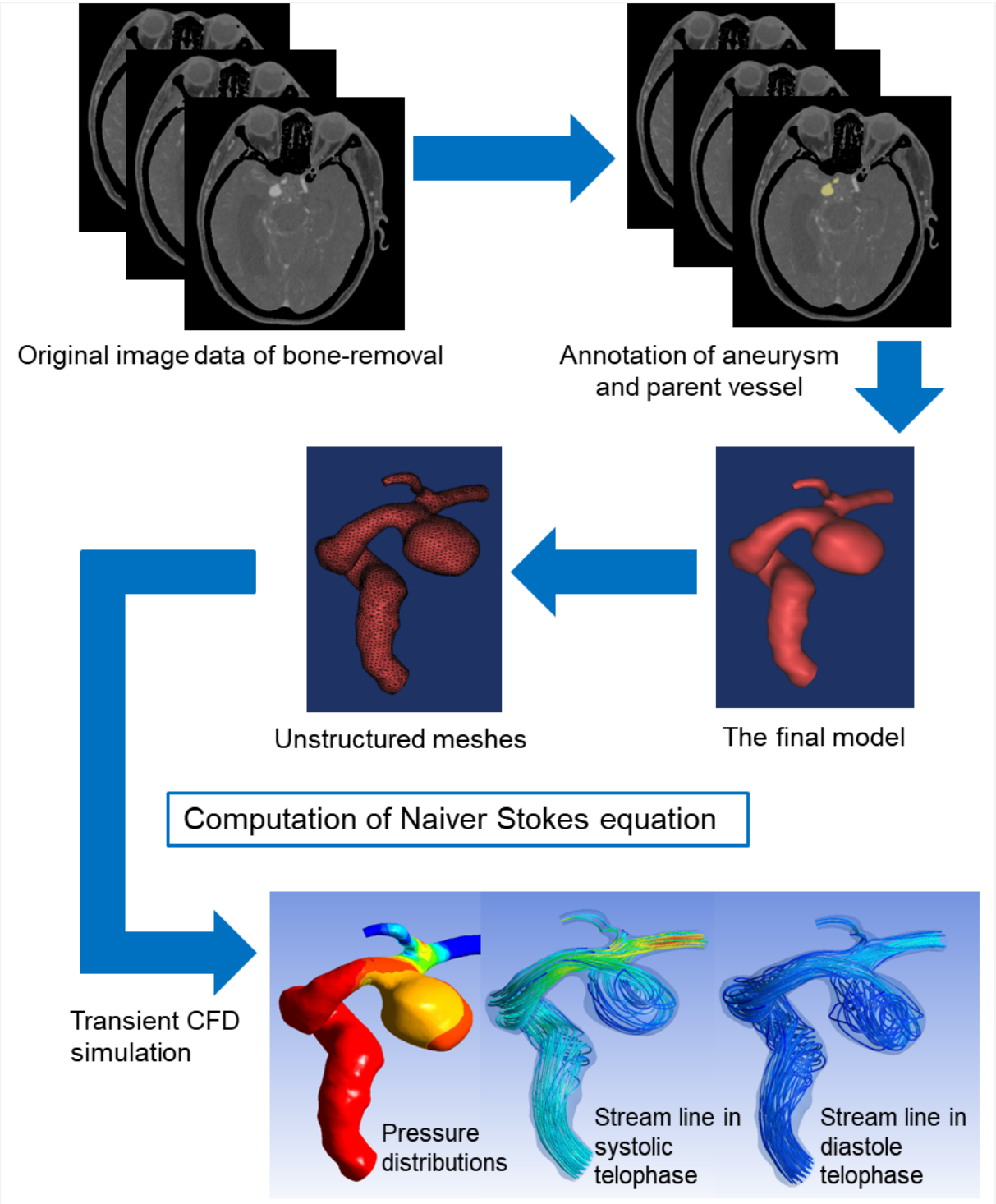

Supplemental Figure 1. Computational Fluid Dynamics (CFDs) Simulation Procedure. The graph indicates the major procedures of CFD, including human annotation, model reconstruction, unstructured meshes, and transient CFD simulation.

Note: The process of the CFD was conducted with commercial software in our study. 2D cross-sectional images of CTA images of the cerebral aneurysms and its parent arteries were first imported into MIMICS, Version 16.0 for image segmentation and reconstruction. The vascular models were converted to a stereolithography (STL) format and exported to

Workbench, Version 15.0 (ANSYS Inc.). Unstructured meshes were created with ICEM CFD, Version 15.0 (ANSYS Inc.). The maximum element size was 0.5 mm with a minimum size of 0.2 mm for the high curvature regions and the surface of the aneurysms. Unsteady CFD simulation was performed with Fluent, Version 15.0 (ANSYS Inc.), which uses a finite volume approach to solve the Navier-Stokes equations (Figure R2, and also seen in Supplemental Figure 1 in the Supplementary file).

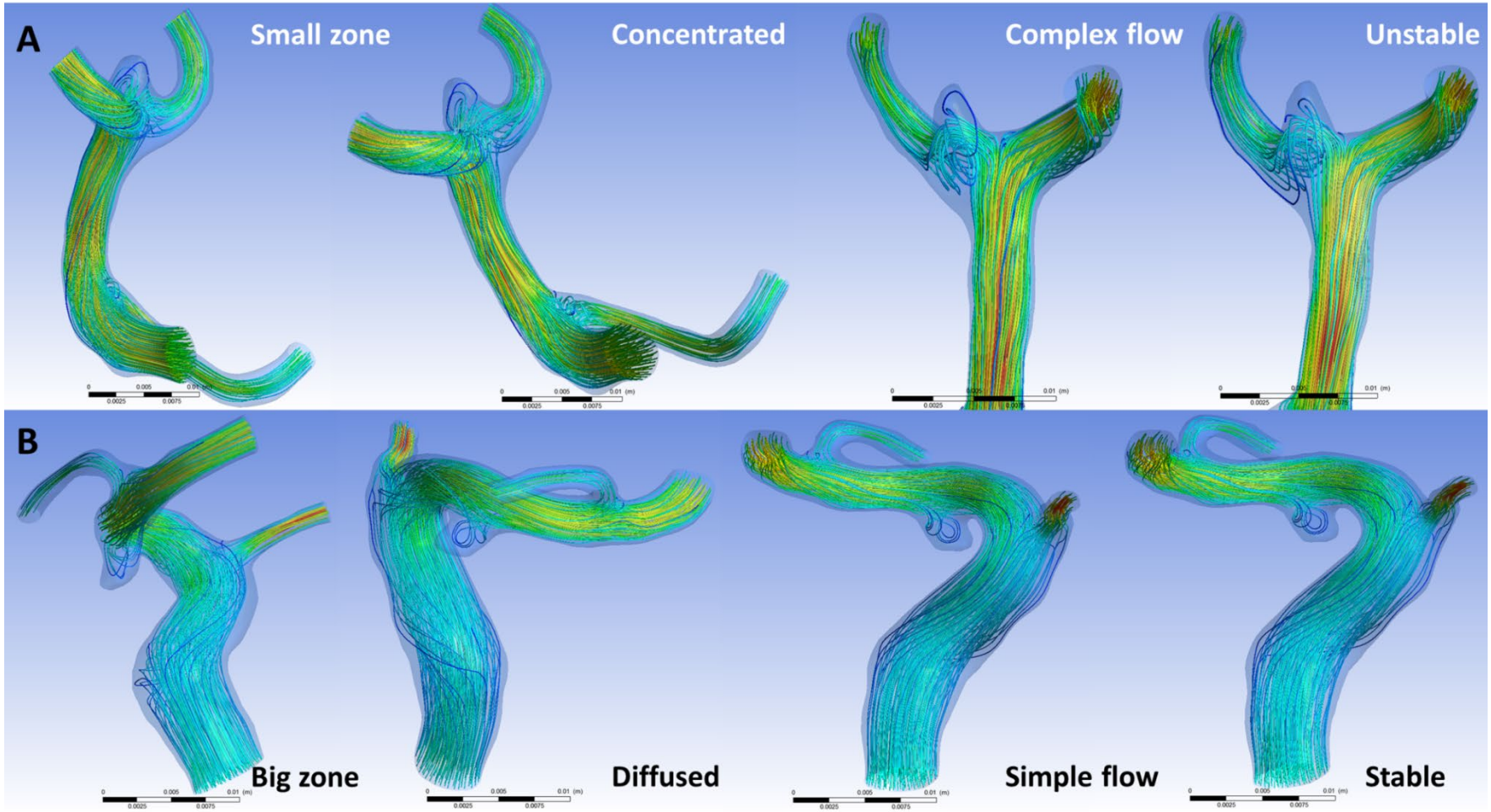

Supplemental Figure 2. Representative Qualitative Hemodynamic Parameters for Unruptured and Ruptured sIAs.

Visualizations of ruptured aneurysm of AcoA (A. top row) and unruptured aneurysm of PcoA (B. bottom row) at peak systole for the first three and at end diastole for the fourth one by using streamlines. From left to right, the visualizations show impingement zone concentration, complexity, and stability.

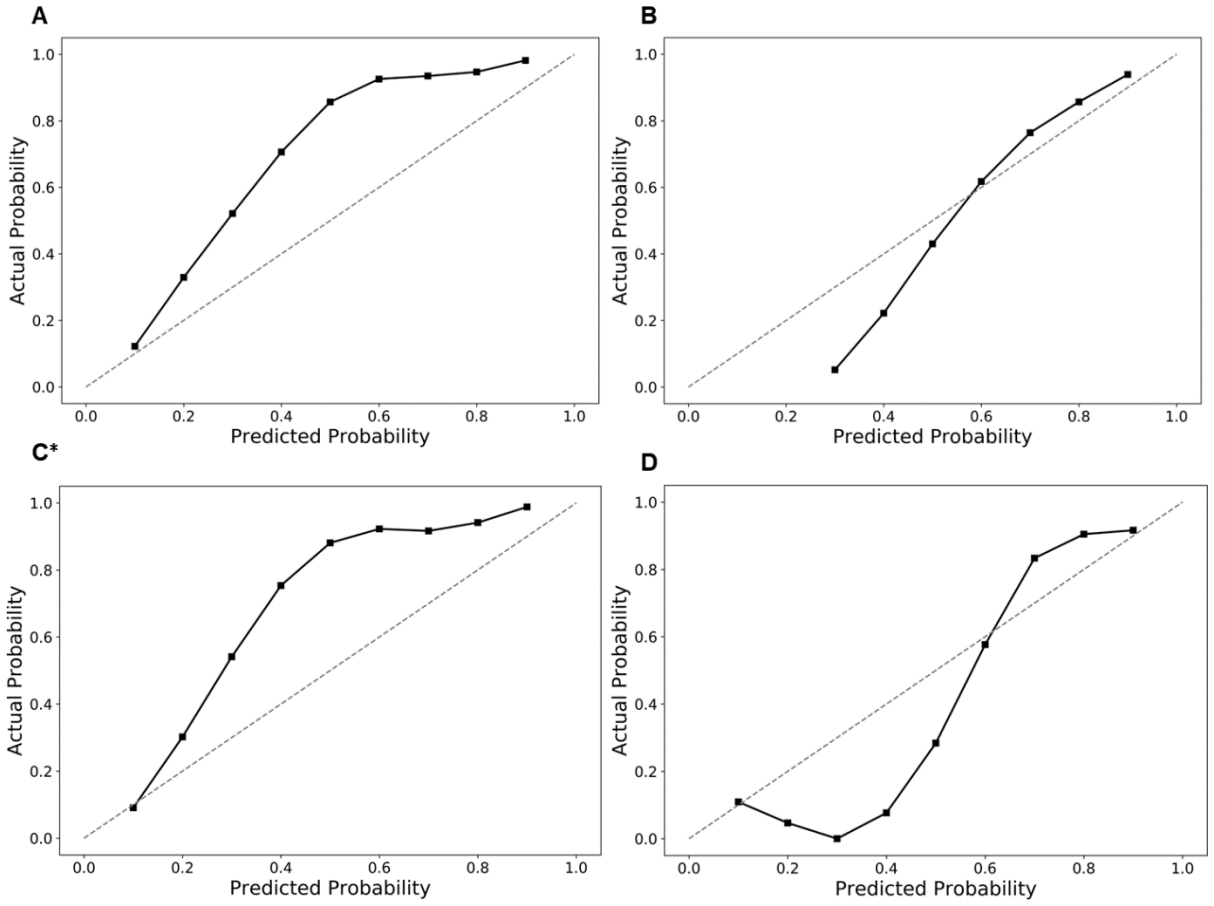

Supplemental Figure 3. Calibration Curves in the Internal Dataset.

Panels A-D: Calibration curves in the internal validation dataset for LR, RF, SVM, and MLP, respectively.

LR, logistic regression model; SVM, support vector machine model; RF, random forest model.

*:The output of each data sample of SVM Model is distance between the hyperplane and data sample, so we first apply sigmoid function on it to transform this distance to a value in range from zero to one to represent the probability.

Note: A (LR) and C (SVM) tend to underestimate the probability of rupture. B (RF), for the interval with low prediction probability, tends to overestimate the probability of rupture; for the interval with high prediction probability, the prediction probability is more accurate. For D (MLP), for the interval with low prediction probability, it tends to overestimate the probability of rupture; for intervals with high prediction probability, the probability of rupture tends to be underestimated.

Several reasons contributed to the low predicted probability of being ruptured. Firstly, we only have 94 cases in the internal validation cohort, which is too small to construct the calibration curve. Secondly, the probability values generated by SVM or other machine learning models

were not calibrated itself. For example, the SVM often shows a sigmoid curve, which is typical for maximum-margin methods.[1]

Reference

1. Niculescumizil A, Caruana R. Predicting good probabilities with supervised learning. International Conference on Machine Learning, 2005: 625-632.

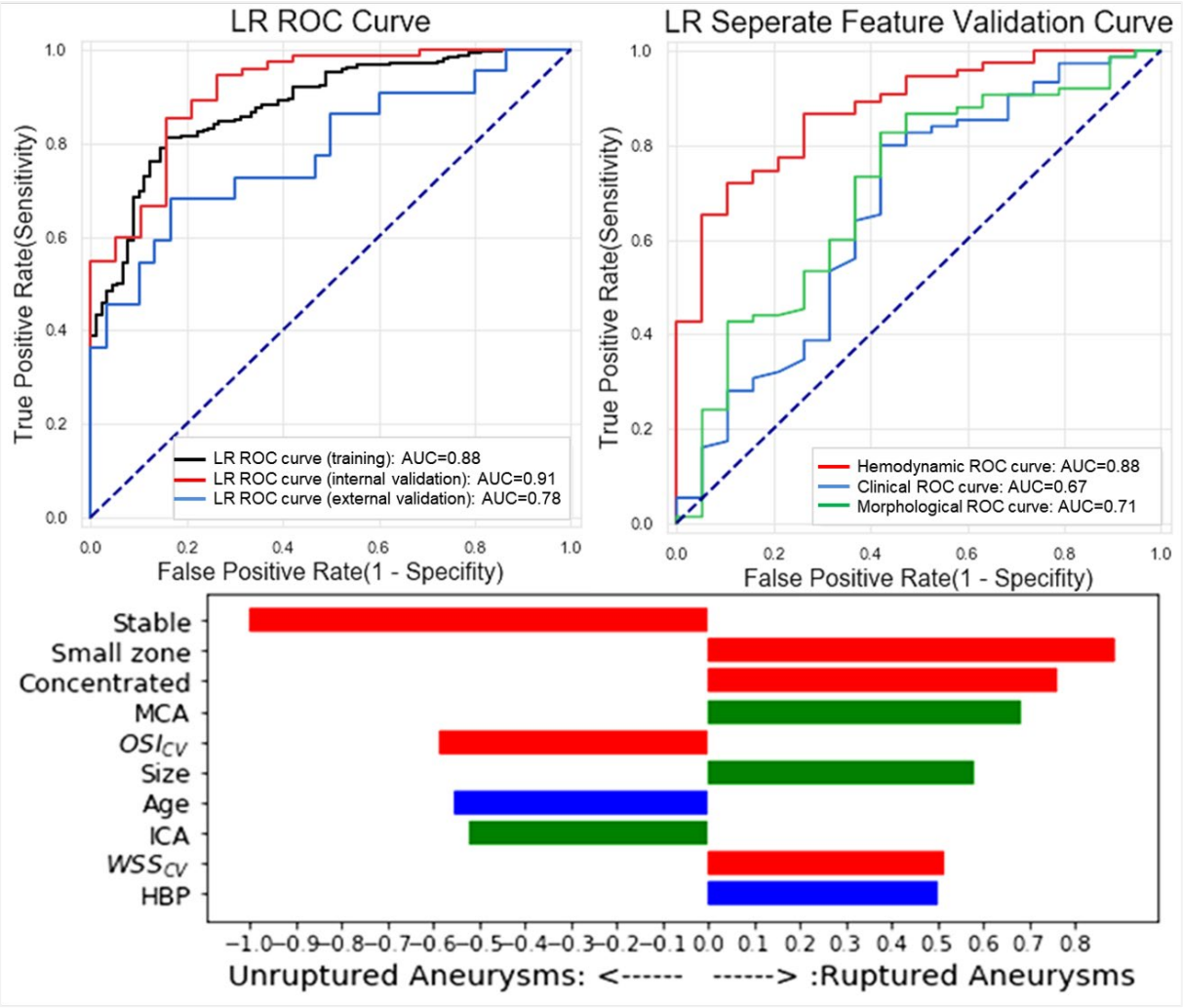

Supplemental Figure 4. Performance of LR algorithm, the derived top 10 variables and the performance of the features belonging to the three categories separately in the internal validation dataset.

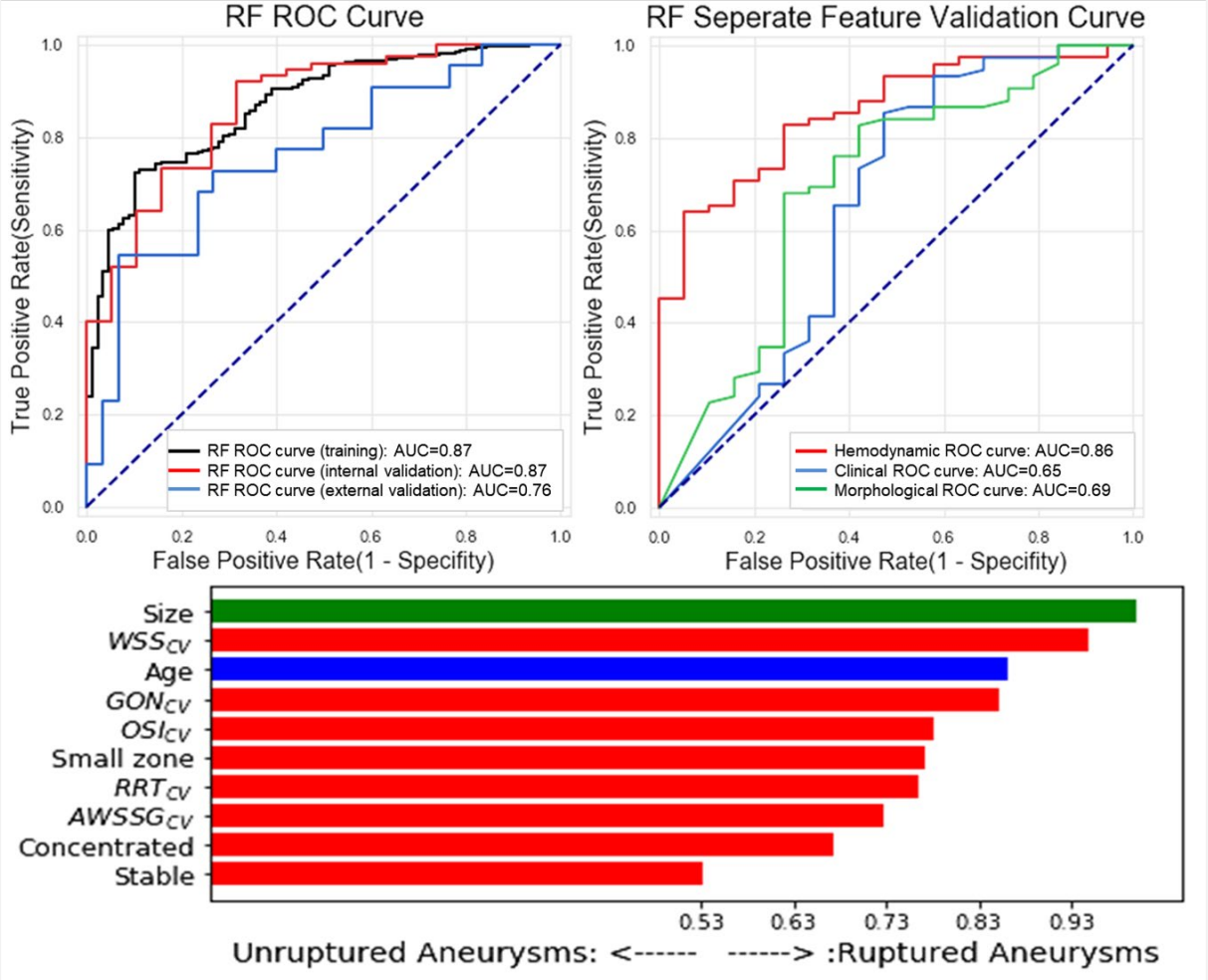

Supplemental Figure 5. Performance of RF algorithm, the derived top 10 variables and the performance of the features belonging to the three categories separately in the internal validation dataset.

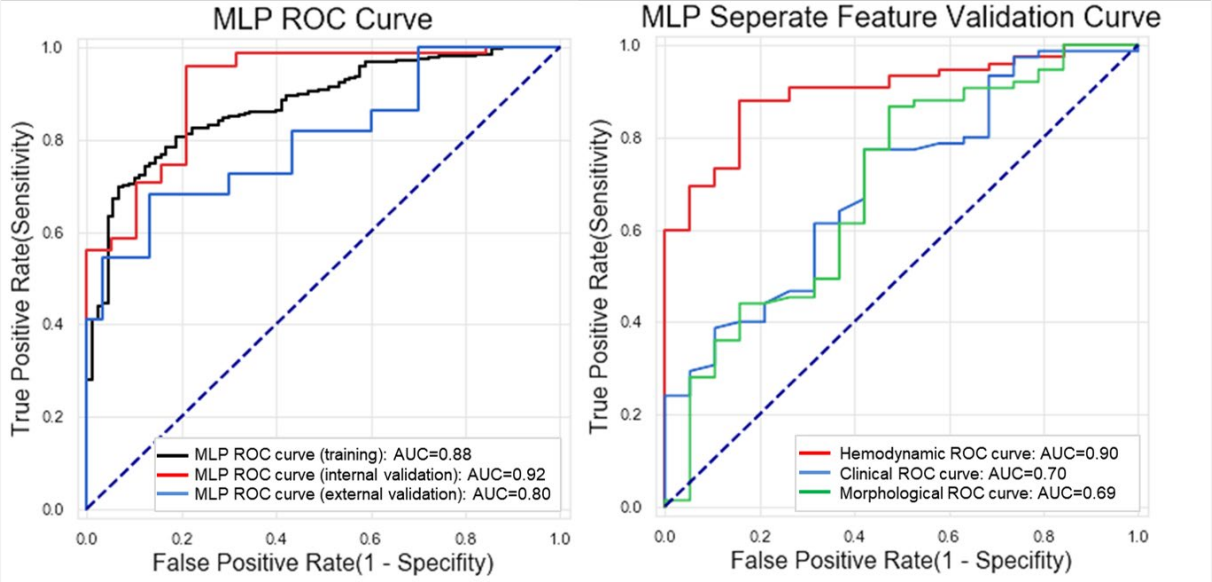

Supplemental Figure 6. Performance of MLP algorithm and the performance of the features belonging to the three categories separately in the internal validation dataset. Note: Feature ranks are not available by MLP.

Supplemental Table 1. CTA Protocols of the Three Medical Centers.

Parameters	Jinling Hospital	Tianjin First Center Hospital	Taizhou Hospital
CT scanners	Somatom Definition Flash or Somatom Definition, Siemens Healthcare, Forchheim, Germany	Revolution CT, GE Healthcare, USA	Somatom Definition Flash, Siemens Healthcare, Forchheim, Germany
tube voltage	120 kVp	100 kVp	100 kVp
tube current	140–180 mAs	SmartmA300-500 NI 5	104 mA
rotation time	0.5 s	0.5 s	0.28 s
CT detector collimation	64 × 0.6 mm or 64 ×2 × 0.6 mm	128 × 0.625mm	128 × 0.6
CM type	Iopromide, Ultravist 300 mg I/mL, Bayer Schering Pharma, Berlin, Germany	Iopromide, Ultravist 370 mg I/mL, Bayer Schering Pharma, Berlin, Germany	Iopromide, Ultravist 370 mg I/mL, Bayer Schering Pharma, Berlin, Germany
CM concentration	300 mg I/ml	370 mg I/ml	370 mg I/ml
CM dosage	60 ml	50 ml	65 ml
CM injection rate	4.0 ml/s	4.5 ml/s	4.5 ml/s
Image matrix	512×512	512 × 512	512 × 512

Field of view	250 mm	250 mm	250 mm
Reconstruction thickness	0.75 mm	0.625 mm	0.75 mm

Supplemental Table 2. Characteristics of Clinical, Morphological and Hemodynamics in Unruptured and Ruptured Small Aneurysms in the Internal Dataset.

Variables	Unruptured group (n=109)	Ruptured group (n=395)	*p*-value
Patient Characteristics			
Age, years	58.3±11.1	54.5±11.8	.003
Male, n (%)	54(49.5%)	150(38.0%)	.030
Single aneurysms, n (%)	94(86.2%)	350(88.6%)	.499
SAH family history, n (%)	0(0.00%)	5(1.3%)	.238
Alcohol intake, n (%)	11(10.1%)	35(8.9%)	.693
Smoking, n (%)	15(13.8%)	41(10.4%)	.320
Hypertension, n (%)	35(32.1%)	171(43.3%)	.036
Diabetes Mellitus, n (%)	9(8.3%)	15(3.8%)	.053
Ischemic stroke, n (%)	9(8.3%)	6(1.5%)	<.001
Coronary artery disease, n (%)	7(6.4%)	5 (1.3%)	.002
Aneurysms Characteristics			
Daughter sac, n (%)	0(0%)	10(2.5%)	.094
Size (mm)	3.68±0.80	3.75 (3.00, 4.35)	.068
Regular shape, n (%)	91(83.5%)	321(81.3%)	<.001
Location			<.001
PCoA, n (%)	31(28.4%)	95(24.1%)	.349

ACoA, n (%)	18(16.5%)	160(40.5%)	<.001
ICA, n (%)	34(31.2%)	31(7.8%)	<.001
MCA, n (%)	11(10.1%)	81(20.5%)	.013
Others, n (%)	15(13.8%)	28(7.1%)	.027
Qualitative Hemodynamic Parameters			
Simple flow, n (%)	73(67.0%)	186(47.1%)	<.001
Concentrated inflow, n (%)	20(18.3%)	243(61.5%)	<.001
Small flow impingement, n (%)	31(28.4%)	290(73.4%)	<.001
Stable flow, n (%)	77(70.6%)	170(43.0%)	<.001
Quantitative Hemodynamic Parameters			
$Pressure_{CV}$ ($\times 10^{-2}$)	0. 78 (0. 42-1.52)	0.58 (0. 21, 1.16)	.018
$AWSSMEAN_{CV}$	0.7580 (0.5867,0.9427)	0.8250 (0.6527, 1.0354)	.006
WSS_{CV}	0.7996 (0.6044, 1.0698)	0.8766 (0.6866, 1.1698)	.005
$AWSSABS_{CV}$	0.7316 (0.5728, 0.9290)	0.7980 (0.6313, 1.0101)	.002
OSI_{CV}	2.1378±0.6034	1.8842±0.5803	<.001
RRT_{CV}	1.1130 (0.8321, 1.3070)	1.1011 (0.8478, 1.3492)	.642
$WSSG_{CV}$	1.3028 (1.0968, 1.5403)	1.3980 (1.1405, 1.7250)	.027
$AWSSG_{CV}$	1.2802 (1.0700, 1.4338)	1.2937 (1.0960, 1.5380)	.138
AFI_{CV}($\times 10^{-1}$)	0.670 (0.366, 1.213)	0.873 (0.409, 1.730)	.035
G_{CV}	1.3252 (1.1342, 1.4864)	1.3479 (1.1546, 1.6132)	.088
GON_{CV}	1.2345 (1.1625, 1.2865)	1.2008 (1.1192, 1.2760)	.013

SAH, subarachnoid hemorrhage; ACoA, anterior communicating artery; ICA, internal carotid artery; PCoA, posterior communicating artery; ACA, anterior cerebral artery; CV, coefficient of variable; WSS, wall shear stress; AWSSMEAN, average of the mean WSS; AWSSABS, averaged WSS-absolute; OSI, oscillatory shear index; RRT, relative residence time; WSSG, WSS gradient; AWSSG, averaged WSS gradient; AFI, aneurysm formation index; G, spatial WSS gradient; GON, Gradient

oscillatory number.

Supplemental Table 3. Characteristics of Patients, Aneurysms and Hemodynamics in the Training, Internal Validation and External Validation Dataset.

Characteristics	Training set (n=410)	Internal validation set (n=94)	$p^{\dagger}$-value	External validation set (n=52)	$p^{\ddagger}$ -value
Patient Characteristics					
Ruptured aneurysms, n (%)	320 (81.0%)	75 (79.8%)	.712	22 (42.3%)	<.001
Age, years	55.6±12.1	54.2±10.1	.302	53.3±11.9	.208
Male, n (%)	166 (40.5%)	38 (40.4%)	.991	20 (35.5%)	.779
Single aneurysm, n (%)	360 (87.8%)	84 (89.4%)	.675	43 (82.7%)	.299
SAH family history, n (%)	5 (1.2%)	0(0%)	.282	0 (0%)	.424
Alcohol intake, n (%)	37 (9.0%)	9 (9.6%)	.867	5 (9.6%)	.889
Smoking, n (%)	43 (10.5%)	13 (13.8%)	.353	7 (13.5%)	.516
Hypertension, n (%)	165 (40.2%)	41 (43.6%)	.549	16 (30.8%)	.188
Diabetes Mellitus, n (%)	20 (4.9%)	4 (4.3%)	.798	1 (1.9%)	.366
Ischemic stroke, n (%)	13 (3.2%)	2 (2.1%)	.592	1 (1.9%)	.621
Coronary artery disease, n (%)	10 (2.4%)	2 (2.1%)	.858	5 (9.6%)	.006

Aneurysms Characteristics					
No daughter sac, n (%)	401 (97.8%)	93 (98.9%)	.479	44 (84.6%)	<.001
Size (mm), n (%)	3.83 (3.25, 4.48)	3.89 (3.12, 4.24)	.519	3.89±0.74	.540
Regular shape, n (%)	265 (64.6%)	56 (59.6%)	.358	32 (61.5%)	
Location			.682		.022
PCoA, n (%)	102 (24.9%)	24 (25.5%)	.895	5 (9.6%)	.014
ACoA, n (%)	142 (34.6%)	36 (38.3%)	.503	14 (26.9%)	.269
ICA, n (%)	55 (13.4%)	10 (10.6%)	.469	19 (36.5)	<.001
MCA, n (%)	77 (18.8%)	15 (16.0%)	.523	12 (23.1%)	.460
Others, n (%)	34 (8.3%)	9 (9.6%)	.688	2 (3.8%)	.260
Qualitative Hemodynamic Parameters					
Simple flow, n (%)	208 (50.7%)	51 (54.3%)	.538	17 (32.7%)	.014
Concentrated inflow, n (%)	214 (52.2%)	49 (52.1%)	.991	8 (15.4%)	<.001
Small flow impingement, n (%)	258 (62.9%)	63 (67.0%)	.457	21 (40.4%)	.002
Stable flow, n (%)	201 (49.0%)	46 (48.9%)	.988	9 (17.3%)	<.001

Quantitative Hemodynamic Parameters					
$Pressure_{CV,}$ ($\times 10^{-2}$)	0.62 (0.22, 1.21)	0.70 (0.26, 1.27)	.652	0.86 (0.56, 1.40)	.007
$AWSSMEAN_{CV}$	0.8148 (0.6387, 1.0285)	0.7952 (0.5947, 0.9637)	.168	0.8737±0.3438	.917
WSS_{CV}	0.8711 (0.6647, 1.1357)	0.8368 (0.6308, 1.1331)	.216	0.8606±0.3079	.149
$AWSSABS_{CV}$	0.7894 (0.6229, 1.0011)	0.7608 (0.5730, 0.9464)	.147	0.8647±0.3554	.867
OSI_{CV}	1.9531±0.5888	1.8782±0.6158	.271	2.3117±0.6880	<.001
RRT_{CV}	1.0989 (0.8479, 1.3484)	1.1574 (0.7701, 1.3411)	.602	1.3091±0.4615	.010
$WSSG_{CV}$	1.3916 (1.1353, 1.6975)	1.3169 (1.0968, 1.6346)	.287	1.3828±0.3256	.299
$AWSSG_{CV}$	1.2954 (1.0943, 1.5145)	1.2726 (1.0471, 1.4860)	.318	1.3208 (1.1211, 1.5387)	.431
AFI_{CV}($\times 10^{-1}$)	0.819 (0.415, 1.643)	0.716 (0.339, 1.599)	.594	0.672 (0.328,1.157)	.107
G_{CV}	1.3479 (1.1540, 1.5771)	1.3005 (1.0963, 1.5866)	.312	1.3753 (1.1530, 1.5670)	.636
GON_{CV}	1.2043 (1.1265, 1.2740)	1.2356 (1.1544, 1.2834)	.135	1.2219 (1.1882, 1.2515)	.371

SAH, subarachnoid hemorrhage; ACoA, anterior communicating artery; ICA, internal carotid artery; PCoA, posterior communicating artery; ACA, anterior cerebral artery; CV, coefficient of variable; WSS, wall shear stress; AWSSMEAN, average of the mean WSS; AWSSABS, averaged WSS- absolute; OSI, oscillatory shear index; RRT, relative residence time; WSSG, WSS gradient; AWSSG, averaged WSS gradient; AFI, aneurysm formation index; G, spatial WSS gradient; GON, Gradient oscillatory number.

†: p <.05 means a significant difference exists in the training dataset and the internal validation dataset.

‡: p <.05 means a significant difference exists in the training dataset and the general external validation dataset.

Supplemental Table 4. Characteristics of Clinical, Morphological and Hemodynamic in Internal Dataset and the Separating External Validation Dataset.

Variables	Jinling dataset (n,504)	Taizhou validation set (n,22)	P# value	Tianjin validation set (n,30)	P* value
Demographic Information					
Ruptured aneurysms, n (%)	395 (78.4%)	11(50.0%)	.002	11 (36.7%)	<.001
Age, years	55.3±11.8	49.2±7.8	.002	56.4±13.6	.635
Male, n (%)	204(40.5%)	5 (22.7%)	.096	15 (50.0%)	.303
Single aneurysm, n (%)	444(88.1%)	16 (72.7%)	.033	27 (90.0%)	.754
SAH family history, n (%)	5 (1%)	0 (0%)	.639	0 (0%)	.584
Alcohol intake, n (%)	46 (9.1%)	0 (0%)	.138	5 (16.7%)	.173
Smoking, n (%)	56 (11.1%)	0 (0%)	.098	7 (23.3%)	.044
Hypertension, n (%)	206 (40.9%)	5 (22.7%)	.089	11 (36.7)	.649
Diabetes Mellitus, n (%)	24 (4.8%)	0 (0%)	.295	1 (3.3%)	.719
Ischemic stroke, n (%)	15 (3.0%)	0 (0%)	.412	1 (3.3%)	.911
Coronary artery disease, n (%)	12 (2.4%)	0 (0%)	.465	5 (16.7%)	<.001

Aneurysms Characteristics					
Size, mm	3.9 [3.2, 4.4]	3.7±0.8	.577	4.0±0.7	.164
Regular shape, n (%)	230(58.2 %)	11(50.0%)	.193	21(70.0%)	.485
Daughter sac, n (%)	10(2.0%)	7(31.8%)	<.001	1(3.3%)	.614
Location			.143		.047
ACoA, n (%)	178(35.3%)	3(13.6%)	.036	11(36.7%)	.881
ICA, n (%)	65(12.9%)	12(54.5%)	<.001	7(23.3%)	.104
PCoA, n (%)	126(25.0%)	3(13.6%)	.226	2(6.7%)	**.022**
MCA, n (%)	92(18.3%)	4(18.2%)	.993	8(26.7%)	.252
Others, n (%)	43(8.5%)	0(0%)	.153	2(6.7%)	.721
Qualitative Hemodynamic Parameters					
Simple flow, n (%)	259(51.4%)	10(45.5%)	.586	7(23.3%)	.003
Concentrated inflow, n (%)	263(52.2%)	6(27.3%)	.022	2(6.7%)	<.001
Small flow impingement, n (%)	321(63.7%)	12(54.5%)	.384	9(30.0%)	<.001
Stable flow, n (%)	247(49.0%)	5(22.7%)	.016	4(13.3%)	<.001
Quantitative Hemodynamic Parameters					

$Pressure_{CV}(\times 10^{-2})$	0.63 [0.24-1.212]	0.97±0.61	.120	0.87 [0.63, 2.12]	.025
$AWSSMEAN_{CV}$	0.8122 [0.6332, 1.0150]	0.8316±0.3015	.716	0.9045±0.3737	.659
WSS_{CV}	0.8604 [0.6590, 1.1355]	0.8371±0.2930	.270	0.8166 [0.6720, 1.0347]	.449
$AWSSABS_{CV}$	0.7828 [0.6147, 0.9851]	0.8205±0.2967	.874	0.8972±0.3948	.513
OSI_{CV}	1.94±0.59	2.4573±0.8170	.008	2.2049±0.5667	.017
RRT_{CV}	1.1012 [0.8386, 1.3465]	1.2184±0.4616	.421	1.3756±0.4576	.004
$WSSG_{CV}$	1.3760 [1.1319, 1.6812]	1.3273±0.2953	.208	1.4235±0.3453	.922
$AWSSG_{CV}$	1.2900 [1.0918, 1.5128]	1.3224±0.3047	.840	1.3584 [1.1586, 1.5439]	.153
$AFI_{CV}(\times 10^{-1})$	0.779 [0.402, 1.630]	0.784±0.605	.158	0.678 [0.371, 1.222]	.398
G_{CV}	1.3410 [1.1430, 1.5780]	1.3601±0.3042	.636	1.4090 [1.1846, 1.5689]	.215
GON_{CV}	1.2080 [1.1300, 1.2787]	1.2267±0.0781	.219	1.2043 [1.1742, 1.2457]	.821

SAH, subarachnoid hemorrhage; ACoA, anterior communicating artery; ICA, internal carotid artery; PCoA, posterior communicating artery; ACA, anterior cerebral artery; CV, coefficient of variable; WSS, wall shear stress; AWSSMEAN, average of the mean WSS; AWSSABS, averaged WSS- absolute; OSI, oscillatory shear index; RRT, relative residence time; WSSG, WSS gradient; AWSSG, averaged WSS gradient; AFI, aneurysm formation index; G, spatial WSS gradient; GON, Gradient oscillatory number.

[#]: $p < 0.05$ means a significant difference exists in the Jinling Hospital and Taizhou validation cohorts.

[*]: $p < 0.05$ means a significant difference exists in the Jinling Hospital and Tianjin validation cohorts.

Supplemental Table 5. Performance of 3 ML Models to Predict Rupture Status of Small Aneurysms in the Training, Internal Validation and External Validation Datasets.

	Training set (n=410)	Internal validation set (n=94)	External validation set (n=52)	Tianjin set (n=30)	Taizhou set (n=22)
LR					
AUC	.88	.91	.78	.66	.89
95% CI	.85-.92	.84-.99	.65-.92	.47-.82	.69-.98
Sensitivity	81.3%	84.0%	72.7%	63.6%	81.8%
Specificity	84.4%	84.0%	60.0%	47.4%	81.8%
Delong test	-	-	.09§	-	.09//
RF					
AUC	.87	.86	.76	.62	.90
95% CI	.83-.91	.78-.96	.63-.90	.42-.79	.70-.99
Sensitivity	72.2%	73.3%	59.1%	45.5%	72.7%
Specificity	90.0%	78.9%	76.7%	63.2%	100.0%
Delong test	-	-	.23§	-	.03//

SVM					
AUC	.88	.91	.82	.71	.90
95% CI	.85-.92	.74-.98	.69-.94	.52-.86	.70-.99
Sensitivity	73.4%	77.3%	68.2%	54.5%	81.8%
Specificity	91.1%	84.2%	76.7%	73.7%	81.8%
Delong test	-	-	.21§	-	.15//
MLP					
AUC	.88	.92	.80	.65	.93
95% CI	.84-.91	.84-.96	.67-.90	.46-.82	.73-.99
Sensitivity	69.7%	70.7%	68.2%	45.5%	90.9%
Specificity	93.3%	89.5%	70.0%	63.2%	82.8%
Delong test	-	-	.75§	-	03//

§: p <.05 means a significant difference exists in AUCs of the ML in the internal and external validation dataset.
//: p <.05 means a significant difference exists in AUCs of the ML in Taizhou set and Tianjin set

Supplemental References:

1. Ren Y, Chen GZ, Liu Z, Cai Y, Lu GM, Li ZY. Reproducibility of image-based computational models of intracranial aneurysm: a comparison between 3D rotational angiography, CT angiography and MR angiography. *Biomed Eng Online* 2016;15:50.
2. Can A, Du R. Association of hemodynamic factors with intracranial aneurysm formation and rupture: Systematic review and meta-analysis. *Neurosurgery* 2016;78:510-520.
3. Cebral JR. Mut F, Weir J, Putman CM. Association of hemodynamic characteristics and cerebral aneurysm rupture. *AJNR Am J Neuroradiol* 2011;32:264-270.
4. Breiman, L. Random forests. *Machine Learning* 2001;45:5-32.